The cyclin-dependent kinase 8 module sterically blocks Mediator interactions with RNA polymerase II

Hans Elmlund*†, Vera Baraznenok‡, Martin Lindahl†, Camilla O. Samuelsen§, Philip J. B. Koeck*¶, Steen Holmberg§, Hans Hebert*‖, and Claes M. Gustafsson‡‖

*Department of Biosciences and Nutrition, Karolinska Institutet and School of Technology and Health, Royal Institute of Technology, Novum, SE-141 87 Huddinge, Sweden; †Department of Molecular Biophysics, Lund University, P.O. Box 124, SE-221 00 Lund, Sweden; ‡Division of Metabolic Diseases, Karolinska Institutet, Novum, SE-141 86 Huddinge, Sweden; §Department of Genetics, Institute of Molecular Biology, Oester Farimagsgade 2A, DK-1353 Copenhagen K, Denmark; and ¶University College of Southern Stockholm, SE-141 57 Huddinge, Sweden

Communicated by Roger D. Kornberg, Stanford University School of Medicine, Stanford, CA, August 28, 2006 (received for review February 21, 2006)

CDK8 (cyclin-dependent kinase 8), along with CycC, Med12, and Med13, form a repressive module (the Cdk8 module) that prevents RNA polymerase II (pol II) interactions with Mediator. Here, we report that the ability of the Cdk8 module to prevent pol II interactions is independent of the Cdk8-dependent kinase activity. We use electron microscopy and single-particle reconstruction to demonstrate that the Cdk8 module forms a distinct structural entity that binds to the head and middle region of Mediator, thereby sterically blocking interactions with pol II.

electron microscopy | transcription | protein structure | yeast | *Schizosaccharomyces pombe*

The Mediator complex acts as an interface between gene-specific regulatory proteins and the basal RNA polymerase II (pol II) transcription machinery (1). Mediator functions as a key regulator of pol II-dependent genes in *Saccharomyces cerevisiae* (2), and depletion of human Mediator from nuclear extracts abolishes transcription by pol II (3). The C-terminal domain of pol II (CTD) has an important role for the Mediator function (4, 5), and no fewer than nine *SRB* genes, encoding for Mediator subunits, were originally identified in a screen for mutants that suppress the cold-sensitive phenotype of a CTD truncation mutant (6). In *S. cerevisiae* and *Schizosaccharomyces pombe*, the Mediator complex interacts directly with the unphosphorylated CTD and forms a holoenzyme (5). Based on shape analysis of the low-resolution projection maps, the *S. cerevisiae* Mediator structure has been divided into three compact and visually distinguishable modules: head, middle, and tail domains of approximately equal mass (7).

The subunit composition of *S. cerevisiae* Mediator has been studied in detail, and 21 proteins are bona fide members of the core Mediator complex (1, 8, 9). In addition, a subgroup of Srb proteins, Med12/Srb8, Med13/Srb9, Cdk8 (cyclin-dependent kinase 8)/Srb10, and CycC/Srb11, forms a specific module (the Cdk8 module) that is variably present in Mediator preparations (10, 11). The smaller, core Mediator (S Mediator) lacking the Cdk8 module has a stimulatory effect on basal transcription *in vitro* (5, 12). The larger form of Mediator (L Mediator), containing the Cdk8 module, instead represses basal transcription *in vitro*, and genetic analysis also indicates that the Cdk8 module is involved in the negative regulation of genes *in vivo* (13).

The Cdk8 module influences pol II interactions with Mediator, and only S Mediator can interact with pol II and form a holoenzyme complex (11). The molecular mechanism by which the Cdk8 module negatively regulates pol II interactions has not been clarified, but it has been hypothesized that the negative effect of the Cdk8 module on eukaryotic transcription is caused by Cdk8-dependent phosphorylation of CTD. The hyperphosphorylated form of CTD would bind less tightly to Mediator, which may result in dissociation of pol II from the holoenzyme complex (14, 15).

Here, we use the *S. pombe* system to investigate the molecular basis for the distinct functional properties of S and L Mediator. We find that the Cdk8 module binds to the pol II-binding cleft of Mediator, where it sterically blocks interactions with the polymerase. In contrast to earlier assumptions, the Cdk8 kinase activity is dispensable for negative regulation of pol II interactions with Mediator. It should be noted that the structure and function of Mediator appears conserved in fungi and metazoan cells, and to simplify comparisons with other experimental systems, throughout this study we use the recently proposed unifying Mediator nomenclature (16).

Results

Electron Microscopy of the *S. pombe* Mediator and pol II Holoenzyme. The S Mediator, L Mediator, and pol II holoenzyme are all large enough for meaningful 3D reconstruction from electron micrographs of individual particles. We adsorbed the S and L Mediator preparations to carbon-coated grids before negative staining and imaging in the electron microscope. Although the S Mediator preparation contains pol II, the images revealed only S Mediator devoid of pol II, and we concluded that the specimen preparation induced a dissociation of holoenzyme complexes into free S Mediator and pol II (Fig. 1 *Bottom*). The free S Mediator particles all existed in a characteristic compact conformation that was distinctly different from the appearance of free *S. cerevisiae* pol II in projection (17), which allowed for manual selection of 950 S Mediator particles and calculation of an initial density in EMAN (18). The generated model was used together with the density of pol II in a supervised classification scheme (19) to sort the free S Mediator particles into a homogeneous group before further processing. To validate the classification, we repeated the procedure using our final S Mediator density, which resulted in matching only 450 of 2,400 particles in the S Mediator population to pol II.

In the negatively stained L Mediator preparation, Mediator in complex with the Cdk8 module existed as a fully preserved, stable complex on the grid (Fig. 1 *Middle*). For both the S and L Mediator preparations, we used principal component analysis and examined the negatively stained single-particle populations to obtain information about the angular distribution so that we could choose a suitable method for 3D reconstruction (Fig. 5, which is published as supporting information on the PNAS web site). As noted above, negative stain did not allow us to observe preserved holoenzyme particles, and we

Author contributions: H.E., S.H., H.H., V.B., and C.M.G. designed research; H.E. and V.B. performed research; C.O.S. contributed new reagents/analytic tools; H.E., M.L., P.J.B.K., and S.H. analyzed data; and H.E., H.H., and C.M.G. wrote the paper.

The authors declare no conflict of interest.

Abbreviations: pol II, RNA polymerase II; CTD, C-terminal domain of pol II.

‖To whom correspondence may be addressed. E-mail: hans.hebert@csb.ki.se or claes.gustafsson@ki.se.

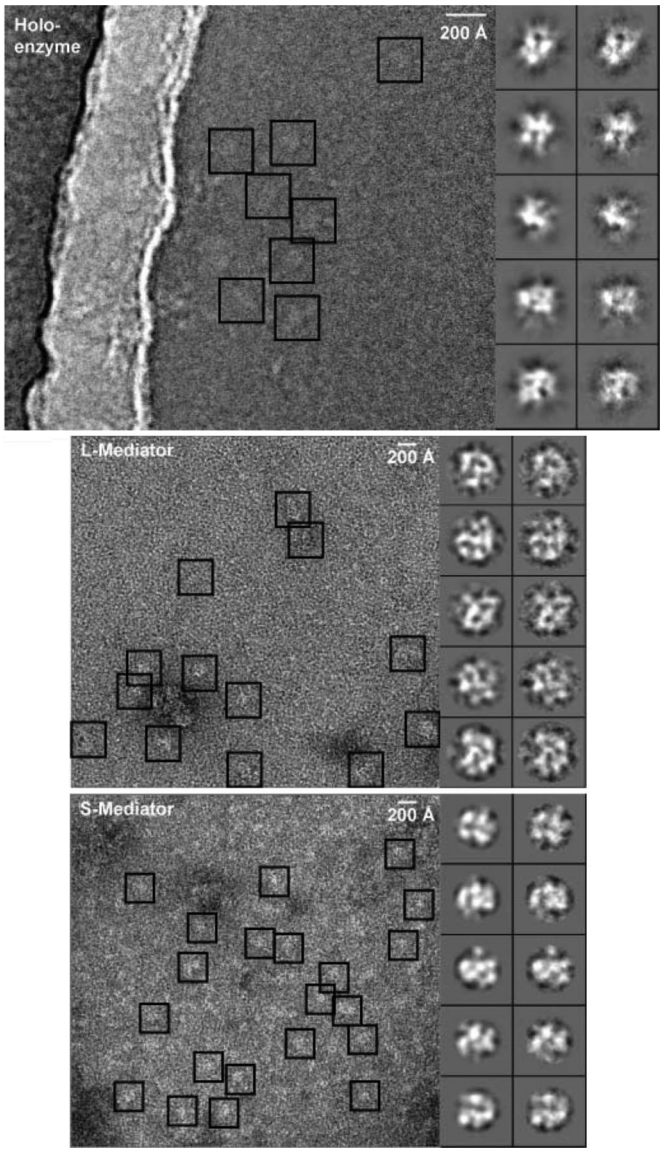

Fig. 1. Typical experimental images, projections, and corresponding reference-free class averages from the Mediator single-particle populations. (*Top*) Holoenzyme particles are seen frozen in a vitreous ice layer. (*Middle*) The L Mediator image shows that Mediator in complex with the Cdk8 module exists as a fully preserved, stable complex on the grid. (*Bottom*) The S Mediator–pol II association is a reversible process; the boxed particles in the S Mediator image are dissociated, free S Mediator particles. Each pair of signal-enhanced images compares a reference-free class average (right) with the corresponding projection from the refined 3D reconstruction (left). The pairs reveal equivalent structural features that indicate that the reconstructions have reached global minima.

therefore prepared vitrified specimens for the pol II holoenzyme and recorded images with cryo-electron microscopy. The cryo-images of the S Mediator preparation showed particles with a size and shape of the expected preserved holoenzyme complex (Fig. 1 *Top*).

To validate the S Mediator, L Mediator, and holoenzyme structures, we compared projections from the generated 3D models with the corresponding reference-free class averages. We found that the reference-free class averages matched the corresponding projections (Fig. 1; see also Fig. 6, which is published as supporting information on the PNAS web site). The conclusion of an angular continuum for the populations was supported by principal component analysis (see *Supporting Text*, which is published as supporting information on the PNAS web site) and shown in diagrams over the angular distribution of the two first Euler angles for all three populations (Fig. 7, which is published as supporting information on the PNAS web site). The strong similarity between class averages and projections established the quality of the initial classification and 3D alignment and demonstrated that the presented 3D structures were trustworthy representations of the Mediator complex.

The resolution of the *S. pombe* S Mediator, L Mediator, and pol II holoenzyme structures was determined by using a fixed 0.5 Fourier shell correlation threshold value. The Fourier shell correlation was calculated between two models by using one half of the data set for each in a simple even–odd test (20), which resulted in a resolution of ≈25 Å for all of the complexes.

Architecture of the *S. pombe* Mediator Structures. The free S Mediator structure possessed two distinct domains of approximately equal mass, with one domain folded toward one side of the other (Fig. 2*A*). The structural appearance was similar to how the middle domain folds toward the head in the structure of *S. cerevisiae* core Mediator (7). This interpretation is supported by the observation that *S. pombe* Mediator complexes contain orthologues to components of the *S. cerevisiae* Mediator head and middle region but lack orthologues to the proteins found in the *S. cerevisiae* tail region (21). In the holoenzyme form, S Mediator undergoes a jackknife-like conformational change to adopt an extended conformation and make room for the globular density of pol II (Fig. 3). The behavior is similar to what has been reported for the *S. cerevisiae* holoenzyme (7). The conspicuous shape of the subcomplex Rpb4/7 in the complete pol II structure (17) made it possible to unambiguously dock the *S. cerevisiae* polymerase into the low-resolution *S. pombe* holoenzyme (Fig. 3 *A–C*). S Mediator associates with the face of pol II opposite of the DNA-binding channel, thus allowing the CTD and the RNA exit region to be fully accessible to the solvent. Rigid-body docking of the S Mediator head (Fig. 3*E*) and middle (Fig. 3*F*) domain into the holoenzyme density demonstrated an excellent fit of the assigned regions. The behavior of the head and middle regions was similar to what was observed in the *S. cerevisiae* holoenzyme, and multiple interactions were observed between pol II and both of the S Mediator domains. The hinge connecting the middle parts of S Mediator with the head is ill defined in the holoenzyme map, presumably due to the high flexibility of the region (Fig. 3*C*).

The Cdk8 Module Sterically Blocks Mediator Interactions with pol II. The 3D appearance of the *S. pombe* L Mediator showed a striking resemblance to the S Mediator structure (Fig. 2*B*). Despite the independence of the 3D reconstructions, we could readily identify S Mediator as a subcomplex of L Mediator. The Cdk8 module formed a coherent additional density located at the entry of the pol II-binding cleft (Fig. 2 *B* and *C*). Compared with the dramatic changes that the *S. pombe* S Mediator has to undergo during formation of the holoenzyme (Fig. 3), the binding of the Cdk8 module only induced a subtle conformational change in the head region, as indicated with arrows in the difference map (Fig. 2*C*). The Cdk8 module covers areas of the head and may in this way hinder specific pol II interactions. This finding is in agreement with reports of direct interactions between Med13 and the head region protein Med17 (9). Furthermore, the Cdk8 module places an extending unit in the pol II-binding pocket, interacting with both the head and the middle regions and presumably resulting in an alignment of the middle parts with the head (Fig. 2*B*). The Cdk8 module therefore appears to form a molecular lid

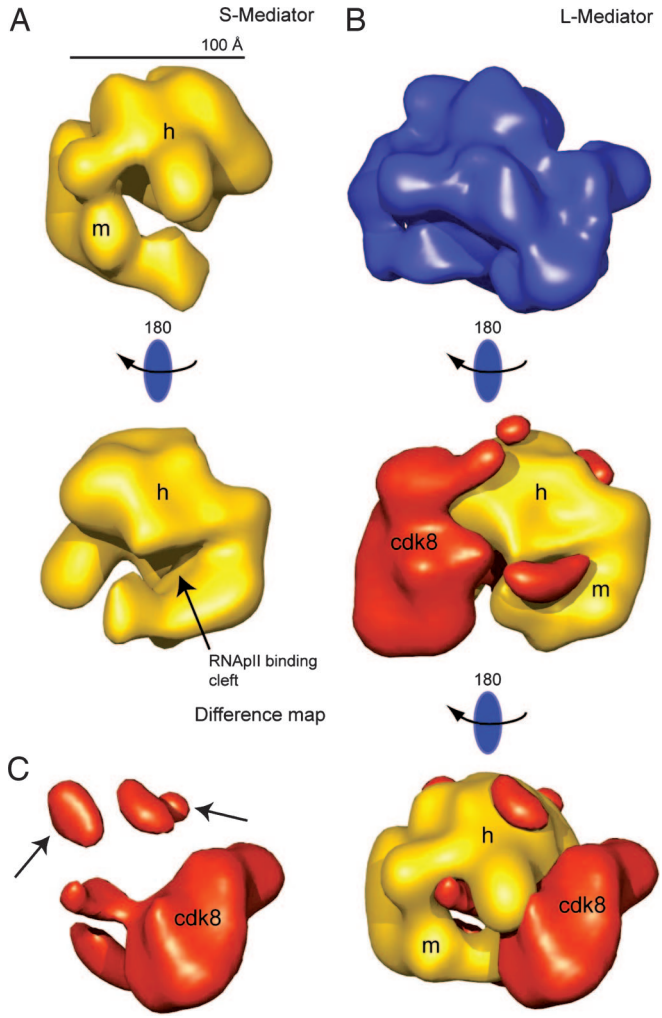

Fig. 2. 3D reconstructions of S and L Mediator at 25-Å resolution. (*A*) In the S Mediator structure, the middle unit (m) folds toward the head (h) and forms a deep cleft, which is the main site for pol II interactions. (*B*) Upon association with the core Mediator, the Cdk8 module interacts primarily with the head, covering the pol II-binding cleft (indicated). The Cdk8 module forms a continuous support around large areas of the Mediator head, except for a submodule binding to the intersection of the head and middle regions, presumably aligning the middle parts with the head and thus locking the L Mediator in a distinctly closed conformation. (*C*) Conformational changes between S and L Mediator are observed exclusively in the head region, as indicated with arrows in the difference map (red).

that covers important pol II-binding surfaces within Mediator and locks the complex in a closed conformation.

CDK8 Kinase Activity Is Not Required for the Cdk8 Module to Prevent pol II Interactions. Our structural characterization of L Mediator suggested that Cdk8 kinase activity is not required to inhibit interactions between pol II and Mediator. To further investigate this possibility, we inactivated Cdk8 kinase activity *in vivo* by mutation of an aspartate residue to alanine at position 158 ($Cdk8^{mut}$). The L Mediator was purified from a $cdk8^{mut}$ strain, and a CTD phosphorylation assay was used to show that the Cdk8 kinase activity was indeed absent from the mutant preparation (Fig. 4*A*). The pol II association with Mediator isolated from the WT and $cdk8^{mut}$ strains was subsequently monitored with immunoblotting. As expected, pol II did not associate with L Mediator isolated from the WT cells (Fig. 4*B*). Notably, pol II was also absent in L Mediator isolated from the $cdk8^{mut}$ strain. We conclude that the physical presence of the Cdk8 module is sufficient to prevent Mediator interactions with pol II, whereas the Cdk8 kinase activity is dispensable.

Discussion

Structural comparisons of different eukaryotic Mediator complexes are limited to overall 3D shape analysis, because only low-resolution electron microscopy models are available. Two distinct conformational states of the yeast Mediator have been reported: the compact conformation associated to the free core Mediator particle and the elongated conformation induced by pol II binding (7, 22–25). *S. pombe* S Mediator lacks a tail module and therefore appears more compact than the previously reported structures. Apart from this difference, *S. pombe* Mediator behaves similarly to the *S. cerevisiae* complex both in its free form, with the head and middle domains closely folded toward each other to form a deep cleft (Fig. 2), and in complex with pol II, with S Mediator in its fully elongated conformation (Fig. 3).

The major interactions observed between *S. pombe* Mediator and pol II are with the Rpb1 subunit (Fig. 3). The front lobe of the head region of S Mediator (domain h1) associates with Rpb1 (light green in Fig. 3) and also with the smaller Rpb8 subunit (gray). Another part of the head region (domain h4) stretches toward the region of Rpb1 where the last-ordered CTD residues (light green atomic surface in Fig. 3) are located. Together with h3, the h4 domain forms a distinct cleft, and it is tempting to speculate that this cleft could be a binding surface for the nearby CTD. Contacts between Rpb1 and Mediator domains have also been reported for the *S. cerevisiae* holoenzyme, in which parts of the Mediator head also contact the ''wall'' domain of Rpb2 (7). In contrast to these findings, we do not observe Mediator interactions with Rpb2 in the *S. pombe* holoenzyme structure. Rpb3 and Rpb11 (Fig. 3) interact with the middle domain of S Mediator, which is in agreement with the findings in *S. cerevisiae* (7).

The dissociable Cdk8 module is not present in the published structures of yeast and murine Mediators, but structures of both a large (23) (TRAP or ARC-L, including the Cdk8 module) and a smaller (26) (CRSP, not including the Cdk8 module) form of human Mediator have been published. Whereas *S. pombe* S and L Mediator have a simple structural relationship with the coherent Cdk8 module as the only structural discrepancy, the 3D appearance of the large and small human Mediator forms diverge significantly. It is possible that the presence of the Cdk8 module induces a major change in the Mediator tail region, which cannot be observed in the *S. pombe* Mediator complex, because it lacks this region. In addition, there is an additional subunit in S Mediator, Med26 (Crsp70), that is absent from L Mediator and therefore may contribute to the dramatic structural differences observed between the two complexes (24). An orthologue to Med26 has not been identified in the yeast Mediator.

Different models have been proposed to explain the repressive function of the Cdk8 module on Mediator-dependent transcription. Cdk8 has been shown to phosphorylate the transcription factor TFIIH and thereby inhibit phosphorylation of CTD, which is required for promoter escape (27). Alternatively, Cdk8 has been shown to directly phosphorylate CTD before formation of the preinitiation complex and thereby inhibit transcription initiation (14). The data presented here reveal another mechanism: The Cdk8 module sterically blocks pol II interactions and may thereby repress transcription initiation (Fig. 4*C*). The physical presence of the Cdk8 module block is sufficient to block pol II interactions, which explains why the kinase activity of Cdk8 is not required.

The structure of L Mediator suggests that the Cdk8 module must be actively displaced before S Mediator may interact with

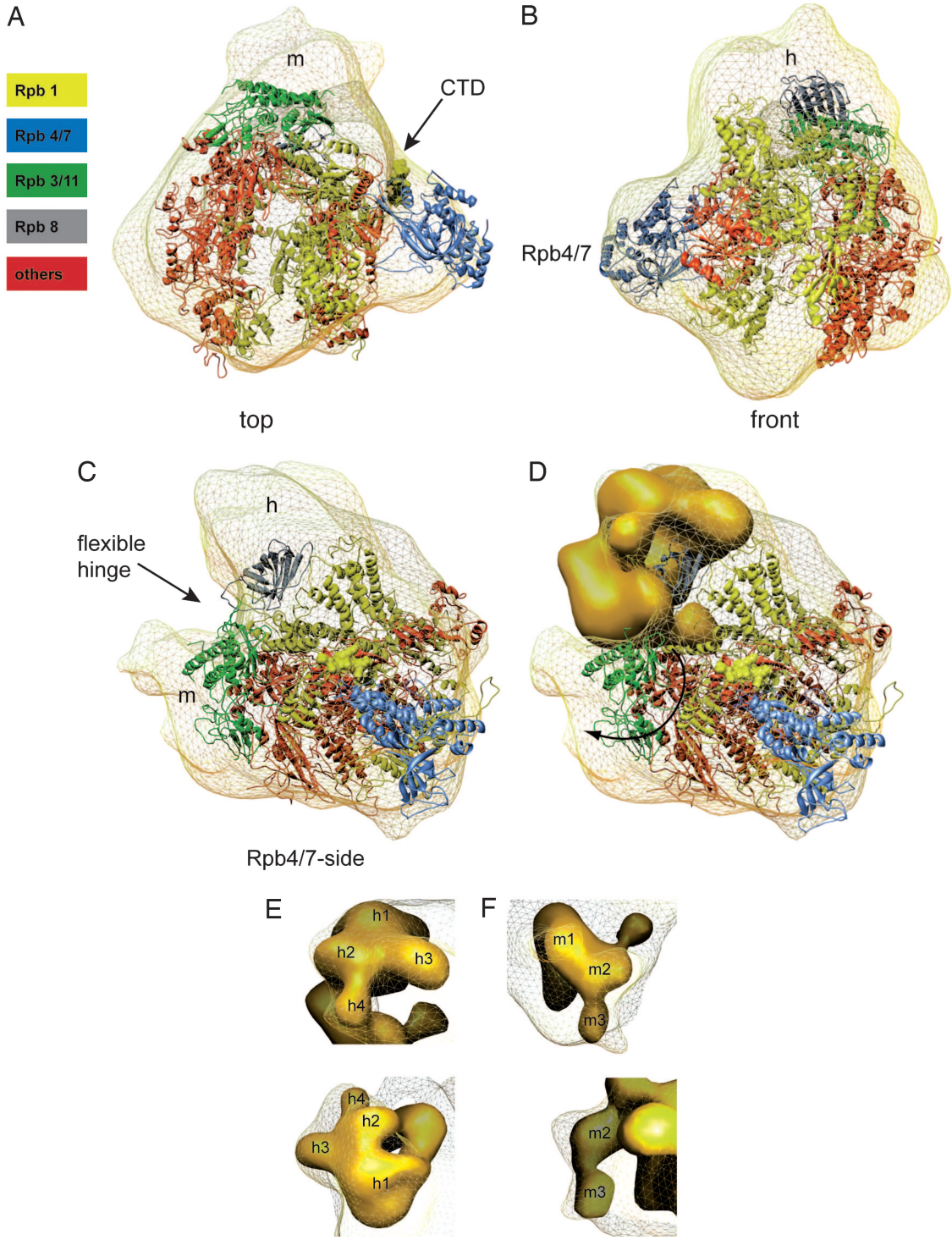

Fig. 3. Cryoelectron microscopy structure of the *S. pombe* pol II holoenzyme with the atomic coordinates of *S. cerevisiae* pol II and the corresponding domains of the S Mediator density docked. (*A* and *B*) The complete *S. cerevisiae* pol II structure with its subcomplex Rpb4/7 (Protein Data Bank ID code 1WCM) was docked into the low-resolution *S. pombe* holoenzyme. The orientation of pol II corresponds to the top (*A*) or front (*B*) view as defined in ref. 17. (*B* shows the Rbp4/7 side view.) (*C*) To better visualize the conformational change in Mediator, the holoenzyme is depicted in a side view, revealing the head (h) and middle (m) domains of S Mediator. (*D*) The free S Mediator (solid structure) has to undergo a jackknife-like conformational change (black arrow) to be able to enfold the globular density of the pol II core. The truncated CTD of the largest subunit of pol II is represented as an atomic surface in *A*–*D*. (*E*) Rigid-body docking of the S Mediator head domain (solid structure) into the holoenzyme density (caged structure). Subdomains of the head region (h1–h4) identified in the 3D reconstructions of both S Mediator and the pol II holoenzyme are indicated. (*F*) Rigid-body docking as in *E* but with the S Mediator middle domain. Subdomains of the middle region (m1–m3) identified in the 3D reconstructions of both S Mediator and the pol II holoenzyme are indicated.

pol II. This model would be in agreement with previous speculations that the Cdk8 module plays a general role in transcription regulation and that this submodule is present in all nonactivated Mediator complexes. How the Cdk8 module is actively displaced from L Mediator during the formation of the pol II holoenzyme remains to be studied.

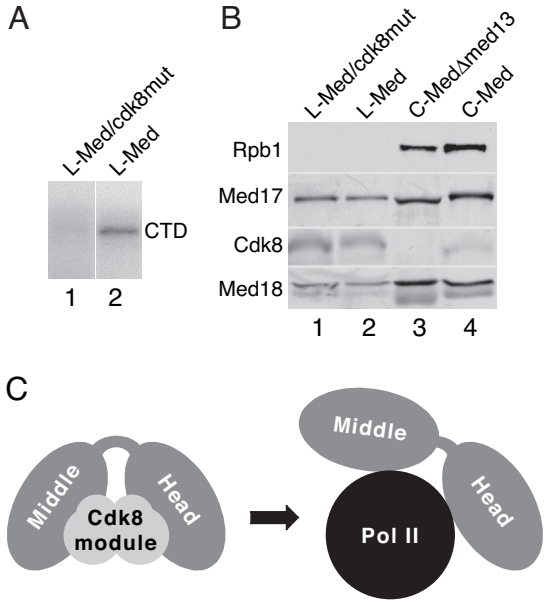

Fig. 4. Cdk8 kinase activity is not required to block pol II interactions with Mediator. (*A*) *In vitro* CTD kinase activity of L Mediator and L Mediator/cdk8^{mut}. (*B*) WT and mutant Mediator complexes purified over IgG-Sepharose. Fractions were separated by 12% SDS/PAGE and immunoblotted with antibodies directed against the indicated proteins. (*C*) A simplified model for the structural relationship between L Mediator and the pol II holoenzyme.

Materials and Methods

Immunoblot Analyses. Immunoblot analysis for Med17 and Med18 was performed as described in ref. 21. Recombinant *S. pombe* Cdk8 (amino acids 2–293) fused to GST was overproduced in *Escherichia coli* BL21 (DE3) pLysS cells (Stratagene, La Jolla, CA) and purified from inclusion bodies as described in ref. 28. The purified GST-Cdk8 protein was used to immunize rabbits (AgriSera, Vännäs, Sweden). pol II was detected with the *8WG16* antibody (Santa Cruz Biotechnology, Santa Cruz, CA).

Protein Purification and Identification. *S. pombe* strains TP33 (h^- Δ*med13*::*G418*^{R}) and TP43 (h^- *ade6-M216 med7*$^+$::*TAP*) are described in ref. 11. The TP46 strain (h^+ *ade6-M216 med7*$^+$::*TAP*) was obtained from the same transformation as TP43. Strain TP161 for purification of the Δ*med13* holoenzyme (lacking the Cdk8 module) was made by crossing TP46 with TP33. L Mediator was purified from the TP68 strain (h^+ *ade6-M216 med13*$^+$::*TAP*). To create the site-directed aspartic-acid-158-to-alanine mutation in Cdk8 (cdk8mut), overlap extension PCR was used, and the PCR fragment was cloned into the pGEM-T Easy Vector System I (Promega, Madison, WI). The resulting plasmid was digested with ApaLI-NheI before transformation of the JY423 strain (29). The obtained strain, TP192, was highly flocculent, and this phenotype was used to score the *cdk8* dead kinase mutant allele in further crossings to create TP313 (h^+ *ade6-M216 cdk8mut med13*$^+$::*TAP*).

For purification of Mediator, 15 liters of *S. pombe* cells was grown to OD_{600} = 3.0–4.0 in yeast extract supplement medium supplemented with 0.2 g/liter adenine (30). Cells were collected by centrifugation (JA-10; Beckman Coulter, Fullerton, CA) at 2,500 rpm and 4°C for 7 min , washed once with ice-cold water, and frozen in liquid nitrogen. Cells were broken in a Freezer/Mill 6850 (SPEX CertiPrep, Metuchen, NJ) by using the following program: 10 min of precooling and seven cycles with 2 min of beating and 2 min of rest at stringency 14. Broken cells were suspended in 0.5 ml of buffer A (250 mM KOH-Hepes, pH 7.8/15 mM KCl/1.5 mM $MgCl_2$/0.5 mM EDTA/15% glycerol/0.5 mM DTT/protease inhibitors) per gram of cell pellet. After the supernatant was cleared by centrifugation (in the JA-10 at 9,000 rpm and 4°C for 15 min), 1/9 vol of 2 M KCl was added and stirred for 15 min. After ultracentrifugation (Ti45, Beckman Coulter) at 42,000 rpm and 4°C for 25 min, 500 μl of IgG beads (1 ml of slurry) (GE Healthcare, Uppsala, Sweden) was added and incubated for 1 h at 4°C. IgG beads were collected by centrifugation (JA-17, Beckman Coulter) at 1,000 rpm and 4°C for 2 min, loaded into a column, and washed with 30 ml of IgG buffer (10 mM Tris·HCl/150 mM KOAc or 150 mM NaCl, pH 8.0). After washing with 25 ml of tobacco etch virus (TEV) protease cleavage buffer (10 mM Tris·HCl/150 mM NaCl/1 mM DTT/0.5 mM EDTA/0.05% Nonidet P-40, pH 8.0), Mediator was eluted by incubation for 1 h at 16°C with 250 units of TEV protease in 2 ml of TEV buffer.

Cdk8 Kinase Assay and *in Vitro* Transcription. The Cdk8 CTD kinase assay was performed as described in ref. 31 with *S. pombe* pol II as the substrate.

Specimen Preparation and Single-Particle Processing. Negatively stained grids were prepared by applying aliquots of the individual S and L Mediator protein preparations (4 μl with an estimated concentration of 0.1 μg/μl) to carbon-coated copper grids that were glow-discharged to facilitate adhesion of the molecules and aid staining by making the film more hydrophilic. Approximately 1 min after adsorption, the excess buffer was blotted, and two washes with water for 25 s were followed by one wash with 1% uranyl acetate for 40 s. Vitrified specimen for cryo-electron microscopy of the holoenzyme preparation was prepared by applying aliquots of the solution (3 μl with an estimated concentration of 0.1 μg/μl) to glow-discharged copper grids coated with a thin, holey carbon film (Quantifoil, Jena, Germany) that was subsequently plunge-frozen with a Vitrobot environment control unit (FEI, Eindhoven, The Netherlands) in liquid ethane. Samples were imaged under low-dose conditions by using a CM 120 transmission electron microscope (FEI) fitted with a LaB_6 filament and operating at an acceleration voltage of 120 kV. Image data for the stained S and L Mediator preparations were collected at a magnification of ×63,000 by using a 1,024 × 1,024-pixel CCD camera (TVIPS, Gauting, Germany), and cryo data for the holoenzyme preparation were recorded onto SO-163 film (Kodak, Rochester, NY) at a magnification of ×60,000. The particles were initially picked out by hand and selected according to the molecular mass of the molecules, assuming a density of 0.83 Da/Å^3 and a spherical form. Defocus for the stained populations was held approximately constant at ≈1 μm, and the images were low-pass filtered to the first zero crossing of the contrast transfer function (CTF). Defocus of the holoenzyme images varied from ≈0.5 to ≈3.5 μm to avoid systematic loss of information due to the CTF. Boxing and CTF phase correction of the 4,000 holoenzyme images were performed in the EMAN suite of programs (18). The individual single-particle populations were classified into ≈120 classes representing distinctly different views of the particles (Fig. 6), and initial 3D reconstruction from untilted images of the particles was performed in EMAN (18) without using CTF amplitude correction in the refinement loop. Several models were selected for further processing and used as starting points for model-based optimization of the shift and rotational parameters assigned to each particle image. Images of S Mediator (2,400 images) and L Mediator (2,800 images) were realigned in Strul (32); the Euler angles and origin shifts were determined through a common-line-based correlation search over the entire Euler angle space, with the EMAN reconstructions as references. The final 3D Coulomb potential maps were calculated by using Spider and weighted back projection (20). Surface rendering of the final density maps was carried out with O (33). MolRay (34) was used to create files for ray tracing with POV-Ray. Mesh representations of the structures were generated in UCSF Chimera. Docking was

carried out manually in O, and difference maps were calculated by scaling the maps to the same voxel range and subtracting the appropriate density. The manual docking of the atomic coordinates of pol II into the holoenzyme density was refined in Situs (35).

We thank Dr. John Davey (University of Warwick, Coventry, U.K.) for providing strain JY423 and Ronny Alvang (Karolinska Institutet, Huddinge) for letting us use his software for principal component analysis.

This work was supported by grants from the Swedish Research Council (to C.M.G. and H.H.), the Swedish Cancer Society (to C.M.G.), the Swedish Foundation for Strategic Research (to C.M.G.), the Danish Research Council (to S.H.), the Novo-Nordisk Foundation, and Fabrikant Vilhelm Pedersen og Hustru Legat as recommended by the Novo-Nordisk Foundation (to S.H.). Work at the Swegene Cryo Electron Microscopy Centre was supported by the Knut and Alice Wallenberg Foundation.

1. Myers LC, Kornberg RD (2000) *Annu Rev Biochem* 69:729–749.
2. Thompson CM, Koleske AJ, Chao DM, Young RA (1993) *Cell* 73:1361–1375.
3. Mittler G, Kremmer E, Timmers HT, Meisterernst M (2001) *EMBO Rep* 2:808–813.
4. Kim YJ, Bjorklund S, Li Y, Sayre MH, Kornberg RD (1994) *Cell* 77:599–608.
5. Myers LC, Gustafsson CM, Bushnell DA, Lui M, Erdjument-Bromage H, Tempst P, Kornberg RD (1998) *Genes Dev* 12:45–54.
6. Nonet ML, Young RA (1989) *Genetics* 123:715–724.
7. Davis JA, Takagi Y, Kornberg RD, Asturias FA (2002) *Mol Cell* 10:409–415.
8. Linder T, Gustafsson CM (2004) *J Biol Chem* 279:49455–49459.
9. Guglielmi B, van Berkum NL, Klapholz B, Bijma T, Boube M, Boschiero C, Bourbon HM, Holstege FC, Werner M (2004) *Nucleic Acids Res* 32:5379–5391.
10. Borggrefe T, Davis R, Erdjument-Bromage H, Tempst P, Kornberg RD (2002) *J Biol Chem* 277:44202–44207.
11. Samuelsen C, Baraznenok V, Spahr H, Kieselbach T, Holmberg S, Gustafsson CM (2003) *Proc Natl Acad Sci USA* 100:6422–6427.
12. Spahr H, Khorosjutina O, Baraznenok V, Linder T, Samuelsen CO, Hermand D, Makela TP, Holmberg S, Gustafsson CM (2003) *J Biol Chem* 278:51301–51306.
13. Holstege FC, Jennings EG, Wyrick JJ, Lee TI, Hengartner CJ, Green MR, Golub TR, Lander ES, Young RA (1998) *Cell* 95:717–728.
14. Hengartner CJ, Myer VE, Liao SM, Wilson CJ, Koh SS, Young RA (1998) *Mol Cell* 2:43–53.
15. Bjorklund S, Gustafsson CM (2005) *Trends Biochem Sci* 30:240–244.
16. Bourbon HM, Aguilera A, Ansari AZ, Asturias FJ, Berk AJ, Bjorklund S, Blackwell TK, Borggrefe T, Carey M, Carlson M, *et al.* (2004) *Mol Cell* 14:553–557.
17. Armache KJ, Mitterweger S, Meinhart A, Cramer P (2005) *J Biol Chem* 280:7131–7134.
18. Ludtke SJ, Baldwin PR, Chiu W (1999) *J Struct Biol* 128:82–97.
19. Valle M, Sengupta J, Swami NK, Grassucci RA, Burkhardt N, Nierhaus KH, Agrawal RK, Frank J (2002) *EMBO J* 21:3557–3567.
20. Frank J, Radermacher M, Penczek P, Zhu J, Li Y, Ladjadj M, Leith A (1996) *J Struct Biol* 116:190–199.
21. Spahr H, Samuelsen CO, Baraznenok V, Ernest I, Huylebroeck D, Remacle JE, Samuelsson T, Kieselbach T, Holmberg S, Gustafsson CM (2001) *Proc Natl Acad Sci USA* 98:11985–11990.
22. Asturias FJ, Jiang YW, Myers LC, Gustafsson CM, Kornberg RD (1999) *Science* 283:985–987.
23. Dotson MR, Yuan CX, Roeder RG, Myers LC, Gustafsson CM, Jiang YW, Li Y, Kornberg RD, Asturias FJ (2000) *Proc Natl Acad Sci USA* 97:14307–14310.
24. Taatjes DJ, Naar AM, Andel F, III, Nogales E, Tjian R (2002) *Science* 295:1058–1062.
25. Taatjes DJ, Marr MT, Tjian R (2004) *Nat Rev Mol Cell Biol* 5:403–410.
26. Naar AM, Taatjes DJ, Zhai W, Nogales E, Tjian R (2002) *Genes Dev* 16:1339–1344.
27. Akoulitchev S, Chuikov S, Reinberg D (2000) *Nature* 407:102–106.
28. Cairns BR, Kim YJ, Sayre MH, Laurent BC, Kornberg RD (1994) *Proc Natl Acad Sci USA* 91:1950–1954.
29. Watson P, Davey J (1998) *Yeast* 14:485–492.
30. Alfa C, Fajntes P, Hyams J, McLeod M, Warbrick E (1993) *Experiments in Fission Yeast* (Cold Spring Harbor Lab Press, Cold Spring Harbor, NY).
31. Spahr H, Beve J, Larsson T, Bergstrom J, Karlsson KA, Gustafsson CM (2000) *J Biol Chem* 275:1351–1356.
32. Lindahl M (2001) *Ultramicroscopy* 87:165–175.
33. Jones TA, Zou JY, Cowan SW, Kjeldgaard M (1991) *Acta Crystallogr A* 47(Part 2):110–119.
34. Harris M, Jones TA (2001) *Acta Crystallogr D* 57:1201–1203.
35. Wriggers W, Milligan RA, McCammon JA (1999) *J Struct Biol* 125:185–195.